Multi-objective optimization of a solar-assisted ground-source CO_2 heat pump system for space and water heating using the Taguchi method and utility concept

Thor Alexis Sazon[a], Qian Zhang[a], and Homam Nikpey[a]

[a] University of Stavanger, Stavanger, Norway, thor.a.sazon@uis.no

Abstract:

This work deals with the optimization of a solar-assisted ground-source CO_2 heat pump system using the Taguchi method and the utility concept. Nine control factors were investigated, including the Borehole Heat Exchanger (BHE) length, BHE spacing, BHE number, solar collector (SC) area, tank thermal energy storage volume, BHE-SC mass flow rate, space heating return temperature, heat pump high-side pressure, and heat pump's output temperature. The seasonal performance factor (SPF), levelized cost of heating (LCOH), and the estimated maximum annual ground temperature change (GTC) were chosen as the response factors to evaluate system performance. The system model was developed using Modelica and 27 simulation runs were implemented according to the L_{27} (9^3) Taguchi orthogonal array. Single objective optimizations were first performed using the Taguchi method to determine the parameter combinations that would optimize the SPF, LCOH, and GTC, separately. After that, multi-objective optimization was performed using the combined Taguchi method-utility concept to determine the control factor combination that would give the optimal overall performance when all response factors are considered simultaneously and given equal importance. Single objective optimizations show that the SPF, LCOH, and GTC are individually most sensitive to the target output temperature of the heat pump, the BHE length, and the SC area, respectively. Optimizing the response factors individually resulted in an SPF of 4.2, an LCOH of 0.122 USD/kWh, and a GTC of 100.24%. Multi-objective optimization resulted in a control factor combination that gave an SPF of 3.58, LCOH of 0.165 USD/kWh, and GTC of 100.03%. When optimized, this system exhibited a performance that is almost comparable to that of conventional systems.

Keywords:

Trans-critical CO_2 heat pump; Borehole heat exchanger; Solar thermal; Modelica; Space and water heating; Taguchi method; Utility concept.

1. Introduction

Recent occurrences that have impacted energy security and affordability have provided significant momentum for a transition away from fossil-fuel-based heating. However, much is still to be done since fossil fuels still meet over 60% of the heating energy demand [1].

Heat pumps (HPs) are recognized by the European Union as a key technology for replacing existing gas boilers and reducing the reliance on Russian natural gas [2]. They can facilitate the utilization of low-grade energy to replace the traditional building energy supply with renewable sources and reduce the consumption of high-grade energy, such as electricity and fuels. However, most HPs currently operate using Hydrofluorocarbons (HFCs) as the working fluid [3]. HFCs replaced the once widely-used ozone-depleting Hydrochlorofluorocarbons (HCFCs) and Chlorofluorocarbons (CFCs) because they exhibited similarly good performance, efficiency, low toxicity, and non-flammability. Unfortunately, they are very strong greenhouse gases, some of which are around a thousand times more potent that CO_2 [4]. Recent initiatives, like the EU's F-gases regulation (EC517/2014) and the Kigali amendment to the Montreal Protocol, suggest that HFC production and utilization will be phased down in the coming years [5,6].

The use of natural working fluids has gained more attention recently because they offer a long-term solution to the problems posed by conventional working fluids. Much interest has been given to CO_2 (R744) due to its zero ozone depletion potential, low GWP, non-toxicity, non-flammability, superior thermodynamic properties, and affordability [7]. Lorentzen first proposed the modern use of CO_2 in a trans-critical HP cycle [8]. So far, it has been commercially applied in different sectors, like combined cooling, heating, ventilation, and air conditioning in supermarkets [9], water heating [10], and automotive air conditioning [11].

Air source heat pumps (ASHPs) account for the majority of global sales (60% in 2021) [2]. However, they have the problem of poor low-temperature heating performance and frosting of the heat exchanger [12].

https://doi.org/10.52202/069564-0070

Ground source heat pumps (GSHPs) are considered more efficient for indoor climate control applications since they use the heat from the ground, which remains at a nearly constant temperature. There are already some studies that have investigated the performance of CO_2 GSHPs [13–16].

Some of the challenges of using a GSHP are: (1) its higher installation cost relative to ASHPs due to the need to drill boreholes and install Borehole Heat Exchangers (BHEs) and (2) the difficulty of operating a single-source HP system continuously and efficiently [12]. One way to overcome these is to add another heat source, such as solar collectors (SCs), to allow for shorter BHEs and more operational options.

There are only very few studies that tackled SAGSHPs that use CO_2 as the working fluid. Kim et al. [17] performed simulations that showed how the various operating parameters could affect the performance of a residential solar-assisted ground-source CO_2 heat pump (CO_2 SAGSHP). They showed that the performance of a CO_2 HP can be improved by using solar and geothermal heat sources and it could supply sufficient heat to the space during winter. Choi et al. [18] performed simulations to compare an R22 and a CO_2 SAGSHP. They found that the R22 SAGSHP had a more stable performance and exhibited a higher heating capacity. Both studies considered relatively low temperatures since their systems were only designed for space heating (SH).

Optimizing the design and operation of SAGSHP systems is necessary to maximize its benefits, considering its high initial cost. However, these are quite complex systems, and optimizing them concerning multiple performance indicators would require a heavy simulation workload.

The Taguchi method [19] is an approach that could be employed to reduce the simulation runs needed to optimize systems. It makes use of an orthogonal array (OA) experimental design with a single analysis of variance and utilizes the signal-to-noise (S/N) ratio to assess parameter settings that minimize the sensitivity of system performance to sources of variations. However, the Taguchi method focuses on the optimization of one performance indicator at a time. To optimize systems while simultaneously considering multiple performance indicators, some studies combined the Taguchi method with the utility concept [20]. Some studies on manufacturing and quality engineering have integrated it with the Taguchi method to handle muti-response optimization problems [21,22]. Some studies have applied the Taguchi method with the utility concept on GSHP systems [23–27].

Verma and Murugesan [28] applied the Taguchi method and the utility concept on a conventional SAGSHP system to optimize the BHE length and the SC area for optimum performance. This paper employs the same concept but with a trans-critical CO_2 heat pump instead of a typical sub-critical vapor compression HFC heat pump. The optimization of a CO_2 SAGSHP for simultaneous space and water heating was performed. Different design and operating parameters were optimized using the Taguchi method and the utility concept, considering the seasonal performance factor (SPF), levelized cost of heating (LCOH), and the estimated maximum ground temperature change (GTC) in a year as response factors.

2. System description

The thermal energy system model in this study was developed using Modelica [29] through the Dymola v2021x [30] environment. It includes a CO_2 HP, SCs, BHEs, and tank thermal energy storage (TTES). The CO_2 HP was modeled using the Thermal Systems library v1.6.1 [31] and then calibrated with experimental data; the BHEs were modeled using a modified version of the MoBTES library v2.0 [32]; the SCs and TTES were both modeled with the Buildings library v9.0.0 [33]. Modelica Standard Library (MSL) v4.0.0 was used here.

2.1. The CO_2 solar-assisted ground source heat pump system model

Figure. 1 shows the schematic of the Modelica model of the whole thermal system in this work while the models of the different system components are given in Figure. 2. Verification of the validity of a system model is best done by calibrating it against data from a real-world installation of the exact system. However, since neither the facility nor data is available to the researchers, the system model was built using component models that have been validated or calibrated individually.

The SCs and the BHEs, connected in series, provide the heat input to the CO_2 HP. This configuration was chosen to allow the storage of excess solar energy in the ground. Different studies [34,35] have shown that this configuration results in better performance. When solar irradiation is available, the SC heats the cold water-side fluid coming from the evaporator of the heat pump. The solar-heated fluid is then directed to the BHEs, where it either extracts or injects energy, depending on its temperature relative to the ground. After passing through the BHEs, the fluid then goes to the evaporator of the CO_2 HP.

A controller that varies the rotational speed of the HP's compressor is used to set the temperature of the hot fluid coming from the CO_2 HP. Another controller sets the flow from the bottom of the TTES to ensure that the temperature there does not go below 50°C. This ensures that the temperature in the DHW distribution system is kept higher than the proliferation temperature of Legionella (20 - 45°C) [36]. The used colder fluid

https://doi.org/10.52202/069564-0070

coming from SH, water heating, and from the bottom of the TTES gets recirculated, mixed, and then reheated in the system. The temperature of the fluid after being used for DHW production was set at 10°C since the city water was assumed to be at 7°C. Although not explicitly modeled here, this assumes that the heat exchange process to supply the heat needed for DHW production occurred at a 3°C pinch temperature. The SH return temperature is varied as one of the control factors. The weather of Bergen, Norway, obtained from the EnergyPlus database [37], was used in this work and the demand side was represented by one year of measured hourly thermal demand data.

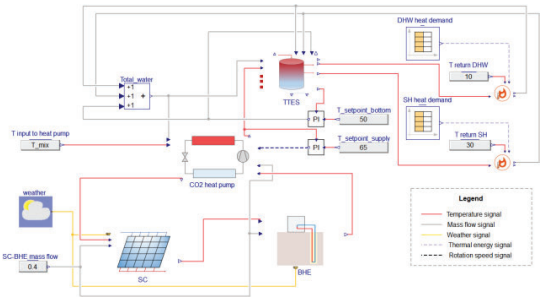

Figure. 1. The CO_2 SAGSHP system model.

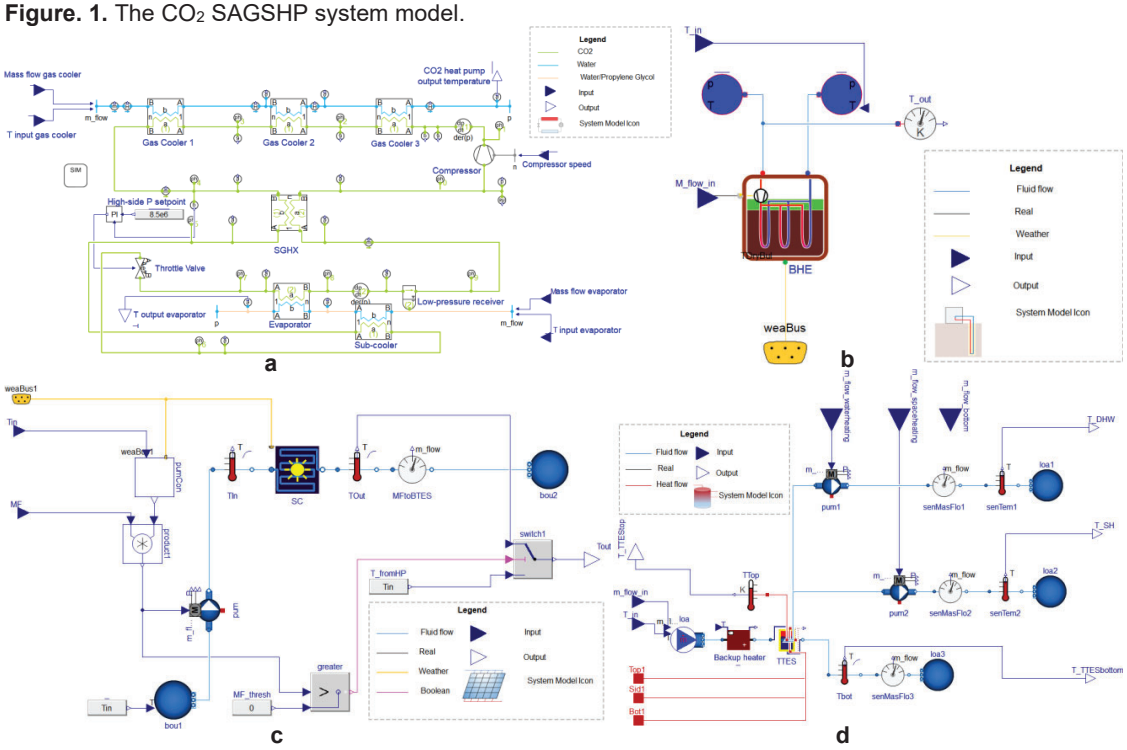

Figure. 2. Component models: (a) CO_2 HP, (b) BHE, (c) SC, (d) TTES.

2.2.1. The CO_2 heat pump model

The CO_2 HP (Figure. 2a), modeled after a 6.5-kW prototype unit [38,39], consists of counter-flow tripartite gas coolers, an evaporator, a compressor, a throttle valve, a suction gas heat exchanger (SGHX), a sub-cooler, and a low-pressure receiver. The throttle valve and the low-pressure receiver function together to control the high-side pressure of the HP [38]. The CO_2 HP model was developed using basic components, such as heat exchangers, valves, and compressors. Thus, it required calibration.

Measured data at the design condition at 85 bars were used to calibrate the model. Available information [38] was used to set the values of some parameters, including the tube diameters of all the tube-in-tube heat exchangers, as well as their weights, material of construction, and length; the size of the low-pressure receiver; and the compressor displacement and operating range. During the calibration, the values of the heat transfer coefficients of every heat exchanger and the efficiencies of the compressor were adjusted until

https://doi.org/10.52202/069564-0070

the model could simulate measured test data (Table 1). The model was calibrated against the data for the high-side pressure P_{GC} = 85 bars, while the other measured data were used to test the calibrated model. Calibration and test errors were obtained by comparing the measured and simulated COPs. The error generated by the calibrated model increases when it is used to simulate the off-design lower high-side pressure. This can be partly attributed to the choice of using a simplified compressor model that assumes constant efficiencies.

Table 1. Calibration of the CO_2 HP unit at ~60°C GC3 output temperature, ~35/30°C GC2 input/output temperature (GC refers the gas coolers; T_E is the evaporator temperature in the CO_2 loop).

Data type	P_{GC} (MPa)	T_E (°C)	Q_{GC1} (W)	Q_{GC2} (W)	Q_{GC3} (W)	Power (W)	Tin/out_{CO2_GC} (°C)	M_{CO2} (kg/s)	COP	Error
Measured*	8.5	-5.1	1608	2942	2357	1775	86.40/9.80	1.441	3.89	-0.26%
Calibrated	8.5	-5.1	1534	2934	2242	1730	86.56/9.80	1.449	3.88	
Measured*	8.98	-5	1550	2596	2801	1878	90.60/8.50	1.442	3.70	1.89%
Simulated	8.98	-5	1480	2637	2594	1779	90.76/8.17	1.417	3.77	
Measured	8.03	-5.1	1674	2728	1828	1699	81.60/18.00	1.440	3.67	4.90%
Simulated	8.03	-5.1	1707	2981	1907	1715	83.82/15.41	1.500	3.85	

*Design conditions

2.2.2. The borehole heat exchanger model

The BHE model (Figure. 2b) was developed using the MoBTES library [32]. MoBTES was originally developed under MSL v3.4, but in this work, it was revised to function with MSL v4.0. The parameters assumed for the BHE are given in Table 2. The ground was assumed to have the characteristics of Slate, one of the common rock types in some parts of Norway [40] while the thermal gradient was assumed to be 0.0125 K/m, similar to that of some wells drilled in Bergen, Norway [41].

Table 2. Summary of BHE parameters.

BHE parameter	Value
Geothermal gradient (K/m)	0.0125
Ground density (kg/m^3)	2760
Ground specific heat (J/kg-K)	920
Ground thermal conductivity (W/m-K)	2.1
BHE type	Single U
Borehole diameter (m)	0.15
Tube inner diameter (m)	0.034
Tube thickness (m)	0.003
Tube thermal conductivity (W/m-K)	0.4
Shank spacing (m)	0.08
Grout density (kg/m^3)	1900
Grout thermal capacity (J/kg-K)	1300
Grout thermal conductivity (W/m-K)	1.5

2.2.3. The solar thermal model

The solar thermal component model (Figure. 2c) was developed using the Buildings library v9.0.0 [33]. The main components used here are the solar pump controller and the SCs. The solar pump controller dictates whether the pump to the SCs is active or inactive depending on the value of the incident solar radiation. The pump is activated when the incident solar radiation is higher than the critical radiation, as defined by [42]:

$$G_{TC} = (F_R U_L (T_{in} - T_{ENV}))/(F_R(\tau\alpha)), \quad (1)$$

where G_{TC} is the critical solar radiation, $F_R U_L$ is the heat loss coefficient, T_{in} is the inlet temperature, T_{ENV} is the ambient temperature, and $F_R(\tau\alpha)$ is the maximum efficiency. When the incident solar radiation is lower than G_{TC}, the fluid bypasses the SCs. The solar collector was modeled according to the EN12975 [43] test data for a glazed flat-plate solar collector WTS-F1-K1/K2 from Max Weishaupt GmbH [44] (Table 3).

Table 3. Summary of SC parameters following the EN 12975 test standard

SC parameter	Value
Area/collector (m^2)	2.32
Dry weight (kg)	42
Fluid volume (m^3)	0.0023
Pressure drop during test conditions (Pa)	100
Mass flow per unit collector area (kg/s-m^2)	0.02
Maximum efficiency	0.802
Heat loss coefficient	3.601
Temperature dependence of heat loss	0.014
Incidence angle modifier	0.97

https://doi.org/10.52202/069564-0070

Nominal solar irradiance in ratings data (W/m^2)	1000
Nominal temperature difference in ratings data (K)	20

2.2.4. The tank thermal energy storage model

The TTES component (Figure. 2d) was also developed using the Buildings library. It uses the stratified storage tank model, which implements several volumes that exchange heat between themselves and with the ambient via conduction. Each volume contains a fluid port that may be used to inject or withdraw water to or from the tank. After passing through a backup heater, hot fluid from the heat pump is injected into the top layer. Relatively cold fluid is drawn from the bottom to manage the temperature inside the tank. Hot water from the top layer and the middle layer are withdrawn to provide the energy required for water heating and SH, respectively.

2.2.5. The thermal demand

Hourly demand data for SH and DHW production from a school in Stavanger, Norway was utilized as the reference of the demand input to this model. The choice of using heat demand and weather data from two different cities was due to data availability. Nonetheless, Stavanger and Bergen are two cities close to one another that have relatively similar climate conditions. The capacity of the system model in this study is limited to ~6.5 - 7 kW since the data used to calibrate the CO_2 heat pump is from a 6.5 - 7kW prototype unit. The demand data from the school is much higher than this so it was normalized, by dividing all data by the measured maximum demand, and then multiplied to 3 kW and 3.5 kW for SH and water heating, respectively (Figure. 3). Peak demands, which comprise less than 1% of the total demand data, were also filtered out for simplicity.

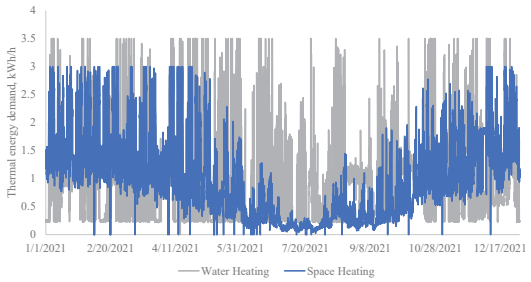

Figure. 3. The thermal energy demand.

3. Methods

The Taguchi method was implemented to determine the runs needed to be simulated, determine the parameters that significantly affect system performance, and determine how to optimize the system concerning individual performance indicators. Multi-objective optimization was then performed by combining the utility concept with the Taguchi method.

3.1. Taguchi method

The Taguchi method is a technique that applies the standard OA to determine the optimal number and set-up of the necessary trial runs for optimization. This allows the determination of the best level of each parameter (control factor) to optimize a given response factor. The first step in this method is the determination of the response factors, the objective functions, the parameters to be considered, and their corresponding levels. In this work, the response factors include the SPF, LCOH, and estimated maximum GTC. The objective is to keep the SPF and GTC high while keeping the LCOH low. Based on the number of control parameters and levels, the OA would be selected. The OA specifies the optimum number of trial runs needed to get maximum information about the system. The minimum number of trial runs to be conducted can be determined by:

$$N_{Taguchi} = 1 + NV(J-1). \quad (2)$$

Where $N_{Taguchi}$ is the minimum number of trial runs, NV is the number of variables, and J is the number of levels. Analysis of the results entails the calculation of the S/N ratio for each run and the analysis of variance (ANOVA). The S/N ratio is a measure of robustness, which is used to identify parameters that reduce process or product variability by minimizing the effects of uncontrollable factors. The S/N ratio of the SPF and GTC were calculated using the higher the better concept (Eq. 3), while the S/N ratio of the LCOH was calculated using the lower the better concept (Eq. 4).

$$Higher\ the\ better\ \frac{S}{N} = -10\ log_{10}\frac{1}{n}\sum_{i=1}^{n}\frac{1}{y_i^2} \quad (3)$$

$$Lower\ the\ better\ \frac{S}{N} = -10\ log_{10}\frac{1}{n}\sum_{i=1}^{n}y_i^2 \quad (4)$$

https://doi.org/10.52202/069564-0070

Where y_i is the raw response factor. ANOVA was used to determine the relative importance of the control factors by computing the percentage contribution of each parameter to the overall response. The degree of freedom (df), the sum of squares (SS), mean squares (MS), significance, and percentage of contribution were all calculated in the analysis.

3.2. The response and control factors

There are 9 control parameters considered, each having 3 levels (Table 4). Given this, an OA with 27 trial runs L_{27} was utilized. A full factorial combination will require 19683 experiments (3^9), which would be too time-consuming and complex. Applying the OA will give the same quality of information with just 27 runs. The BHE length, BHE number, SC area, and TTES volume were chosen since they are known to have a direct relationship with the cost of the system. The BHE spacing was included since it is a way to diffuse the thermal imbalance induced by the system to the ground [25]. The SC-BHE mass flow, CO_2 HP high-side pressure, and HP output temperature were chosen since they are parameters that could easily be controlled. The SH return temperature was included to represent the effects of the efficiency of the distribution system.

Table 4. Control factors investigated and their levels.

Parameter	Label	Level		
		1	2	3
BHE length (m)	A	50	100	150
BHE spacing (m)	B	3	5	7
BHE number	C	4	5	6
SC area (m^2) (number of collectors)	D	6.96 (3)	13.92 (6)	20.88 (9)
TTES volume (m^3)	E	0.5	1	2
SC-BHE mass flow* (kg/s)	F	0.2	0.4	0.8
SH return Temperature (°C)	G	20	30	35
CO_2 HP high-side pressure (MPa)	H	8.5	9.0	10
CO_2 HP output temperature** (°C)	I	60	65	70

*the flow rate of the fluid circulating through the SC, BHE, and the evaporator's waterside
**the temperature of the water as it comes out of the water side of the gas cooler

The values of the different levels of the parameters were determined by running trial simulation runs, some initial sizing calculations, and some operational considerations to ensure that the system would be able to provide the thermal energy demand while keeping the performance at reasonable levels.

The response factors considered in this work are the SPF, LCOH, and GTC. The SPF was calculated by dividing the total energy delivered by the system to the demand for a year by the total energy utilized to run it. The system spends energy to run the compressors and the circulation pumps. The LCOH was calculated by dividing the total cost of the system by its total energy production throughout its lifetime. Note that the electricity cost from 1 year of simulating the operation of the system was assumed to be the cost of the yearly operation. The assumptions used for cost calculations are summarized in Table 5. The GTC was obtained from the BHE model, which gives out the average ground temperature as it is utilized as a heat source or heat sink. The GTC is calculated by dividing the ground temperature after one year of simulation by the initial ground temperature (GTC > 100%: temperature in the ground went up; GTC < 100%: the ground temperature went down). Changes to the GTC were kept minimal, but a higher-the-better concept was applied since the system was designed for heating purposes. SPF, LCOH, and GTC values that are more representative of the long-term performance of the system could be obtained if the model was run for more years. However, because of the relatively big computational load, the simulations were limited to one year only. Trial runs show that the SPF and LCOH do not vary so much. However, the GTC was seen as highest for the first year and substantially declines in the succeeding years, assuming the yearly weather and demand remain similar. Hence, the GTC calculated in this study was assumed to represent the maximum expected temperature decline throughout the lifetime of the system.

Table 5. Summary of parameters used for cost calculations.

Parameter	Value	Reference/Notes
Cost of flat plate SC (EUR/m^2)	632.5	Average of SC costs in [45]
Cost of BHE (EUR/m)	65	[46]
Cost of TTES (EUR/m^3)	1150	Average cost of 0.8 – 2 m^3 TTES [47]
CO_2 Heat pump compressor cost (RMB)	$17547W^{0.4488}$	W is the rated compressor power [48]
CO_2 Heat pump gas cooler cost (RMB)	$1874.4A^{0.9835}$	A is heat exchanger area [48]
CO_2 Heat pump evaporator cost (RMB)	$331.7A^{0.9390}$	A is heat exchanger area [48]
Lifetime of the system (years)	25	[46]
Weighted Average Cost of Capital (WACC)	2%	Weighted Average Cost of Capital (WACC) HP [49]
Exchange rate (USD/EUR)	1/1.01	Exchange rate in Sept. 2022
Exchange rate (USD/RMB)	0.14/1	Exchange rate in Sept. 2022
Exchange rate (NOK/USD)	1/0.0975	Exchange rate in Sept. 2022
Electricity cost (NOK/kWh)	2.4415	Average electricity price in Norway in 2022 [50]

https://doi.org/10.52202/069564-0070

3.3. The utility concept

The utility concept was used to perform multi-response optimization by combining the individual values of the response factors (SPF, LCOH, and GTC) into one unified index called utility [20]. The overall utility function can be expressed as the utility of every performance indicator. Assuming that the performance indicators are independent of one another, the overall utility can be calculated as the sum of individual utilities. Prioritization of the effect of a response factor on the overall utility can be done by introducing a weighting coefficient w_j (Equation 5).

$$U(y_1, y_2, \dots, y_n) = \sum_{j=1}^{n} w_j U_j(y_j) \quad (5)$$

In the utility concept, a preference scale must be set up to represent the lowest and the highest performance. As in previous studies that used the utility concept in thermal energy systems [24–26,28], this study employs a minimum preference number of 0 and a maximum of 9. In a logarithmic scale, the preference number is represented by the formula below so that it has a value of 9 at the optimal level of a performance indicator.

$$U_j(y_j) = P_j = A_j \log \frac{y_j}{y'_j} \;\; with \;\; A_j = \frac{9}{\log \frac{y^*}{y'_j}} \quad (6)$$

Where y'_j is the minimum acceptable value of a performance indicator and y^* is the optimal value of the performance indicator. The overall utility is then calculated by:

$$U = \sum_{j=1}^{n} w_j P_j. \quad (7)$$

4. Results and discussions

The main objective of the study is to optimize a CO_2 SAGSHP system considering 3 performance indicators: SPF, LCOH, and GTC. Taguchi method was performed first to optimize the systems with regard to each performance indicator individually. Afterward, a combination of the Taguchi method and the utility concept was implemented to perform multi-objective optimization, assuming that all response factors are equally important.

4.1. Taguchi method – the orthogonal array and the S/N ratios

Following the Taguchi design concept, an L_{27} orthogonal array was chosen. Each trial run was performed according to the combination of parameters determined by this array to get the values of the response factors and the S/N ratios (Table 6). The S/N ratio values for the SPF and GTC were calculated using the higher-the-better concept while those for LCOH were calculated with the lower-the-better concept. The S/N ratios were then averaged in consideration of the different levels of each control factor (Figure. 4).

Table 6. The Taguchi L_{27} (3^9) standard orthogonal array and the experimental plan.

Trial No.	A	B	C	D	E	F	G	H	I	Response Factors			S/N ratios		
										SPF	LCOH (USD/kWh)	GTC (%)	SPF	TAC	GTC
1	1	1	1	1	1	1	1	1	1	3.52	0.131	99.3208	10.93	17.67	-0.0592
2	1	1	1	1	2	2	2	2	2	3.12	0.141	99.3329	9.88	17.02	-0.0581
3	1	1	1	1	3	3	3	3	3	2.81	0.152	99.329	8.96	16.36	-0.0585
4	1	2	2	2	1	1	1	2	2	3.44	0.154	99.8624	10.73	16.23	-0.012
5	1	2	2	2	2	2	2	3	3	3.15	0.162	99.856	9.95	15.81	-0.0125
6	1	2	2	2	3	3	3	1	1	2.58	0.182	99.8545	8.23	14.81	-0.0126
7	1	3	3	3	1	1	1	3	3	3.36	0.178	100.0275	10.52	15.01	0.0024
8	1	3	3	3	2	2	2	1	1	3.19	0.183	100.0203	10.07	14.75	0.0018
9	1	3	3	3	3	3	3	2	2	2.45	0.208	100.0196	7.78	13.62	0.0017
10	2	1	2	3	1	2	3	1	2	2.6	0.236	99.9384	8.31	12.56	-0.0054
11	2	1	2	3	2	3	1	2	3	2.48	0.241	99.9021	7.88	12.35	-0.0085
12	2	1	2	3	3	1	2	3	1	3.41	0.217	99.9313	10.65	13.26	-0.006
13	2	2	3	1	1	2	3	2	3	2.68	0.226	99.8583	8.56	12.91	-0.0123
14	2	2	3	1	2	3	1	3	1	3.37	0.209	99.833	10.54	13.6	-0.0145
15	2	2	3	1	3	1	2	1	2	2.85	0.225	99.8597	9.1	12.95	-0.0122
16	2	3	1	2	1	2	3	3	1	3.24	0.186	99.9441	10.22	14.63	-0.0049
17	2	3	1	2	2	3	1	1	2	2.72	0.202	99.9427	8.69	13.9	-0.005
18	2	3	1	2	3	1	2	2	3	2.83	0.201	99.959	9.04	13.94	-0.0036
19	3	1	3	2	1	3	2	1	3	2.22	0.313	99.8968	6.92	10.08	-0.009
20	3	1	3	2	2	1	3	2	1	3.38	0.278	99.8915	10.57	11.12	-0.0094
21	3	1	3	2	3	2	1	3	2	3.53	0.276	99.8694	10.95	11.2	-0.0113
22	3	2	1	3	1	3	2	2	1	2.89	0.245	99.9751	9.23	12.21	-0.0022
23	3	2	1	3	2	1	3	3	2	3.24	0.236	99.9989	10.22	12.53	-0.0001
24	3	2	1	3	3	2	1	1	3	2.65	0.256	99.9986	8.46	11.83	-0.0001
25	3	3	2	1	1	3	2	3	2	3.17	0.239	99.9221	10.01	12.42	-0.0068
26	3	3	2	1	2	1	3	1	3	2.35	0.268	99.9424	7.42	11.44	-0.005
27	3	3	2	1	3	2	1	2	1	3.92	0.23	99.9128	11.86	12.75	-0.0076

The combination of the levels that give the highest average S/N represents the optimal setup. Thus, the combination of control factors that gave the optimum SPF is A1B3C1D1E1F1G1H3I1. The effect of a certain control factor on the response factor could be inferred from the difference between the highest and the

https://doi.org/10.52202/069564-0070

lowest value of the S/N ratio. It could be seen that the SPF is most responsive to HP output temperature (I) and least sensitive to the TTES volume (E). Higher SPFs are expected when the target output temperature of the HP (I) is set low because less energy is needed by the compressor to reach a lower output temperature for a given high-side pressure. However, this is limited by the minimum temperature requirements of the DHW and SH distribution systems. Applying the determined control factor combination in simulation resulted in an optimal SPF of 4.2.

The combination of control factors that would give the optimum LCOH is A1B2C1D1E1F1G1H3I1. This resulted in an optimal LCOH of 0.122 USD/kWh, which is comparable to the LCOH of some conventional solar thermal combi HP systems [51]. As expected, optimizing the LCOH requires the reduction of capital and operation expenses, like using shorter and fewer BHEs (C), a smaller SC area (D), a smaller tank (E), a smaller pumping requirement (F), and a lower HP output temperature (I).

For GTC, the optimum parameter combination is A3B3C3D3E1F1G3H1I3. This resulted in an optimal GTC of 100.24%. The GTC is most responsive to the BHE spacing (B) and SC area (D). This means that the reduction of the temperature in the ground could be reduced by increasing the spacing between the BHEs or increasing the solar input to the system. Large solar input could even increase ground temperature, which could be beneficial to the system to some extent. Drilling deeper and more boreholes could also help, albeit would entail higher costs.

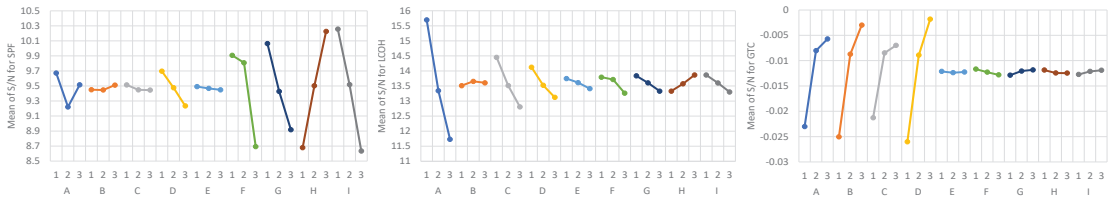

Figure. 4. The Taguchi average S/N ratio for each control parameter for every response factor.

4.2. Taguchi method – ANOVA analysis

ANOVA was used to estimate the relative significance of each parameter in terms of percentage contribution to the overall response (Table 7). The significance denotes which control factors could induce statistically significant effects on the response factor at different confidence levels. As shown, the SPF was most sensitive to the target output temperature of the HP. It is also noticeably more responsive to the operating parameters (F-I) than the design parameters (A-E). The LCOH is most sensitive to the BHE length (A) and number (C) since the BHE is the most expensive component of the system. This shows the influence of capital expenses. Almost all control parameters considered induced statistically significant changes to the LCOH. In contrast to the SPF, the GTC is mostly affected by the design parameters (A-D). The SC area (D) and BHE spacing (B) are shown to be the main contributors to the GTC.

Table 7. The results of the ANOVA for each response factor.

	df	SS	MS	F	Pr(>F)	Significance	Contribution	SS	MS	F	Pr(>F)	Significance	Contribution	SS	MS	F	Pr(>F)	Significance	Contribution
				SPF						LCOH						GTC			
A	2	0.942	0.471	1.817	0.224		2.43%	71.590	35.795	1673.636	0.000	***	75.83%	0.002	0.001	1586.000	0.000	***	20.19%
B	2	0.024	0.012	0.046	0.955		0.06%	0.095	0.048	2.221	0.171		0.10%	0.002	0.001	2357.000	0.000	***	30.00%
C	2	0.027	0.014	0.053	0.949		0.07%	12.285	6.142	287.189	0.000	***	13.01%	0.001	0.001	1112.000	0.000	***	14.15%
D	2	0.963	0.482	1.859	0.217		2.49%	4.564	2.282	106.707	0.000	***	4.83%	0.003	0.001	2786.000	0.000	***	35.46%
E	2	0.009	0.004	0.017	0.983		0.02%	0.513	0.256	11.988	0.004	**	0.54%	0.000	0.000	0.000	0.756		0.00%
F	2	8.183	4.091	15.791	0.002	**	21.13%	1.482	0.741	34.639	0.000	***	1.57%	0.000	0.000	6.000	0.024	*	0.08%
G	2	5.935	2.967	11.453	0.004	**	15.33%	1.156	0.578	27.013	0.000	***	1.22%	0.000	0.000	5.000	0.030	*	0.06%
H	2	10.776	5.388	20.795	0.001	***	27.83%	1.301	0.650	30.413	0.000	***	1.38%	0.000	0.000	2.000	0.170		0.03%
I	2	11.864	5.932	22.895	0.000	***	30.64%	1.430	0.715	33.419	0.000	***	1.51%	0.000	0.000	3.000	0.082	.	0.04%
Residual Error	8	2.073	0.259					0.171	0.021			***		0.000	0.000				

Significance codes: 0 '***' 0.001 '**' 0.01 '*' 0.05 '.'

4.3. Utility-Taguchi – S/N ratios

The utility index for each trial run for every response factor was calculated assuming that all response factors have equal weights (Table 8). The utility index is a number between 0 to 9 that represents the performance of the system (closer to 9 = better performance). The corresponding S/N ratios of the global utility indices were next calculated using the higher-the-better concept. The average S/N ratios are plotted in Figure. 5.

Taking note of the highest S/N ratio for each control parameter gives an optimal parameter combination of A1B3C2D3E2F1G1H3I1. This combination gives the best overall performance of the system. This results in

a global utility index of 6.77 (SPF of 3.58, an LCOH of 0.165 USD/kWh, and a GTC of 100.03%). Compared to a SAGSHP system that uses a conventional working fluid, this optimized system exhibited a slightly lower SPF ($SPF_{conventional}$ = 3.89) [52] and comparable LCOH ($LCOH_{conventional}$ = 0.043 – 0.206 USD/kWh) [51], and GTC (<1°C increase) [52]. Although relatively good performance has been observed, other system or component changes can be explored to further improve its overall performance.

Table 8. The utility indices and their S/N ratios

Trial	SPF utility	LCOH utility	GTC utility	Global utility	S/N ratio global utility
1	6.76	8.41	0.15	5.11	14.16
2	5.32	7.77	0.27	4.45	12.97
3	4.07	7.13	0.23	3.81	11.62
4	6.47	7.00	5.36	6.28	15.96
5	5.42	6.59	5.29	5.77	15.22
6	3.07	5.61	5.28	4.65	13.36
7	6.19	5.81	6.94	6.31	16.00
8	5.58	5.55	6.87	6.00	15.56
9	2.47	4.45	6.86	4.59	13.24
10	3.18	3.40	6.08	4.22	12.51
11	2.60	3.20	5.74	3.85	11.70
12	6.37	4.09	6.02	5.49	14.79
13	3.53	3.75	5.32	4.20	12.47
14	6.23	4.43	5.07	5.24	14.39
15	4.26	3.79	5.33	4.46	12.99
16	5.79	5.43	6.14	5.79	15.25
17	3.70	4.72	6.12	4.85	13.71
18	4.18	4.75	6.28	5.07	14.10
19	1.30	0.98	5.69	2.65	8.47
20	6.26	2.00	5.63	4.63	13.31
21	6.78	2.07	5.42	4.76	13.55
22	4.44	3.06	6.44	4.65	13.34
23	5.78	3.38	6.66	5.27	14.44
24	3.40	2.69	6.66	4.25	12.56
25	5.50	3.27	5.93	4.90	13.81
26	1.97	2.30	6.12	3.47	10.80
27	8.02	3.59	5.84	5.82	15.29

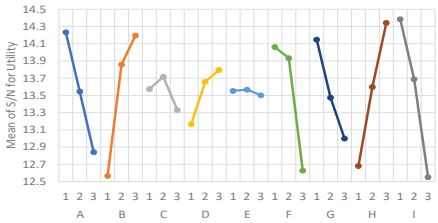

Figure. 5. The Taguchi average S/N ratio for each control parameter for every response factor.

4.4. Utility-Taguchi – ANOVA

As shown in Table 9, the utility index of a CO_2 SAGSHP is most sensitive to the BHE length (A) and least sensitive to the TTES size (E). Relatively significant contributions can also be seen from the output temperature of the HP (I), BHE spacing (B), high-side pressure of the HP (H), and mass flow rate of the fluid circulating through the BHE and SC (F).

Table 9. The results of the ANOVA for the utility index

	df	SS	MS	F	Pr(>F)	Significance	Contribution
			Utility Index				
A	2	25.138	12.569	22.415	0.001	***	22.64%
B	2	18.275	9.138	16.295	0.002	**	16.46%
C	2	2.969	1.485	2.647	0.131		2.67%
D	2	5.879	2.940	5.242	0.035	*	5.30%
E	2	0.053	0.027	0.047	0.954		0.05%
F	2	15.744	7.872	14.038	0.002	**	14.18%
G	2	7.082	3.541	6.315	0.023	*	6.38%
H	2	17.244	8.622	15.376	0.002	**	15.53%
I	2	18.634	9.317	16.615	0.001	***	16.78%
Residual Error	8	4.486	0.561				

Significance codes: 0 '***' 0.001 '**' 0.01 '*' 0.05 '.'

https://doi.org/10.52202/069564-0070

5. Conclusion

A SAGSHP system that utilizes CO_2 as a working fluid was modelled and then optimized in this study using the Taguchi method and the utility concept. The system was first optimized with regards to the SPF, LCOH, and GTC individually using the Taguchi method. Then a combination of the Taguchi method and the utility concept was then applied to perform multi-response optimization, considering the overall performance of the system if the SPF, LCOH, and GTC were deemed of equal importance.

The different combinations of control parameters that optimize the SPF, LCOH, and GTC individually, are A1B3C1D1E1F1G1H3I1, A1B2C1D1E1F1G1H3I1, and A3B3C3D3E1F1G3H1I3, respectively. Applying these set-ups to the model results in an optimal SPF of 4.2, LCOH of 0.122 USD/kWh, and GTC of 100.24%. According to the ANOVA results, the most influential control factors are the HP's target output temperature, the BHE length, and the SC area for the SPF, LCOH, and GTC, respectively.

Combining the Taguchi method with the utility concept allows multi-objective optimization to determine the parameter set-up that will give the optimal overall performance, considering all response factors are weighed equally. By this, the parameter combination that gave the optimal utility index is A1B3C2D3E2F1G1H3I1. This resulted in a 3.58 SPF, a 0.165 USD/kWh LCOH, and a 100.03% GTC. Compared to a SAGSHP system that uses a conventional working fluid, this optimized system exhibited a slightly lower SPF but comparable LCOH. Although relatively good performance has been observed, other system or component changes can be explored to further improve its overall performance. For instance, other system configurations could be examined.

Nomenclature

$F_R U_L$	heat loss coefficient, W/(m² K)	NV	number of variables
$F_R(\tau\alpha)$	maximum efficiency of the solar collector	T_{ENV}	ambient temperature, K
G_{TC}	critical solar irradiation, W/m²	T_{in}	inlet temperature, K
J	number of levels	U	overall utility index
$N_{Taguchi}$	minimum number of Taguchi trial run		

Subscripts and superscripts

C	compressor	DHW	domestic hot water
$CO2$	CO_2 working fluid	E	evaporator
$CO2\_GC$	CO_2 through the gas coolers	GC	gas cooler

References

[1] IEA, "Heating," 2022. Accessed: Feb. 03, 2023. [Online]. Available: https://www.iea.org/reports/heating
[2] IEA, "Heat Pumps," 2022. Accessed: Feb. 03, 2023. [Online]. Available: https://www.iea.org/reports/heat-pumps
[3] BSRIA Ltd., "BSRIA's view on refrigerant trends in AC and Heat Pump segments," Jan. 2020. Accessed: Nov. 14, 2022. [Online]. Available: https://www.bsria.com/uk/news/article/bsrias_view_on_refrigerant_trends_in_ac_and_heat_pump_segments/
[4] K. Onno, "Report Annex 46 HPT-AN46-04: Refrigerants for Heat Pump Water Heaters," Heat Pump Centre c/o RISE – Research Institutes of Sweden, Borås, Dec. 2019. Accessed: Oct. 12, 2022. [Online]. Available: https://heatpumpingtechnologies.org/annex46/wp-content/uploads/sites/53/2020/10/hpt-an46-04-task-1-refrigerants-for-heat-pump-water-heaters-1.pdf
[5] "EU legislation to control F-gases," Jan. 2015. Accessed: Apr. 01, 2022. [Online]. Available: https://ec.europa.eu/clima/eu-action/fluorinated-greenhouse-gases/eu-legislation-control-f-gases_en
[6] United Nations, "The Kigali Amendment (2016): The amendment to the Montreal Protocol agreed by the Twenty-Eighth Meeting of the Parties (Kigali, 10-15 October 2016) | Ozone Secretariat," Oct. 2016. Accessed: Mar. 18, 2021. [Online]. Available: https://ozone.unep.org/treaties/montreal-protocol/amendments/kigali-amendment-2016-amendment-montreal-protocol-agreed
[7] J. Wang, M. Belusko, M. Evans, M. Liu, C. Zhao, and F. Bruno, "A comprehensive review and analysis on CO2 heat pump water heaters," *Energy Conversion and Management: X*, vol. 15, p. 100277, Aug. 2022, doi: 10.1016/j.ecmx.2022.100277.
[8] G. Lorentzen, "Trans-critical vapour compression cycle device," WO1990007683A1, Jul. 12, 1990 Accessed: Feb. 17, 2021. [Online]. Available: https://patents.google.com/patent/WO1990007683A1/en
[9] A. Hafner *et al.*, "Efficient and integrated energy systems for supermarkets," *11th IIR Gustav Lorentzen Conference on Natural Refrigerants: Natural Refrigerants and Environmental Protection, GL 2014*, pp. 311–319, Jan. 2014.

[10] K. Hashimoto, “Technology and Market Development of CO2 Heat Pump Water Heaters (ECO CUTE) in Japan,” IEA Heat Pump Centre Newsletter, 2006. Accessed: Feb. 28, 2023. [Online]. Available: http://waterheatertimer.org/pdf/Market-develop-CO2.pdf
[11] AutomotiveTechinfo, “CO2 as a Refrigerant is Happening,” Jun. 2021. Accessed: Feb. 28, 2023. [Online]. Available: https://automotivetechinfo.com/wp-content/uploads/2021/06/CO2-as-a-Refrigerant-is-Happening.pdf
[12] Z. Han, C. Bai, X. Ma, B. Li, and H. Hu, “Study on the performance of solar-assisted transcritical CO2 heat pump system with phase change energy storage suitable for rural houses,” *Solar Energy*, vol. 174, pp. 45–54, Nov. 2018, doi: 10.1016/j.solener.2018.09.001.
[13] W. Wu, H. M. Skye, and J. J. Dyreby, “Modeling and experiments for a CO2 ground-source heat pump with subcritical and transcritical operation,” *Energy Conversion and Management*, vol. 243, p. 114420, Sep. 2021, doi: 10.1016/j.enconman.2021.114420.
[14] Y.-J. Kim and K.-S. Chang, “Development of a thermodynamic performance-analysis program for CO2 geothermal heat pump system,” *Journal of Industrial and Engineering Chemistry*, vol. 19, no. 6, pp. 1827–1837, Nov. 2013, doi: 10.1016/j.jiec.2013.02.028.
[15] Z. Jin, T. M. Eikevik, P. Nekså, and A. Hafner, “Investigation on CO2 hybrid ground-coupled heat pumping system under warm climate,” *International Journal of Refrigeration*, vol. 62, pp. 145–152, Oct. 2015, doi: 10.1016/j.ijrefrig.2015.10.005.
[16] Z. Jin, T. M. Eikevik, P. Nekså, A. Hafner, and R. Wang, “Annual energy performance of R744 and R410A heat pumping systems,” *Applied Thermal Engineering*, vol. 117, pp. 568–576, May 2017, doi: 10.1016/j.applthermaleng.2017.02.072.
[17] W. Kim, J. Choi, and H. Cho, “Performance analysis of hybrid solar-geothermal CO2 heat pump system for residential heating,” *Renewable Energy*, vol. 50, pp. 596–604, Feb. 2013, doi: 10.1016/j.renene.2012.07.020.
[18] J. Choi, B. Kang, and H. Cho, “Performance comparison between R22 and R744 solar-geothermal hybrid heat pumps according to heat source conditions,” *Renewable Energy*, vol. 71, pp. 414–424, Nov. 2014, doi: 10.1016/j.renene.2014.05.057.
[19] G. Taguchi, *Introduction to Quality Engineering: Designing Quality Into Products and Processes*. Asian Productivity Organization, 1986.
[20] P. Karande, S. K. Gauri, and S. Chakraborty, “Applications of utility concept and desirability function for materials selection,” *Materials & Design*, vol. 45, pp. 349–358, Mar. 2013, doi: 10.1016/j.matdes.2012.08.067.
[21] P. Kumar, P. B. Barua, and J. L. Gaindhar, “Quality optimization (multi-characteristics) through Taguchi’s technique and utility concept,” *Quality and Reliability Engineering International*, vol. 16, no. 6, pp. 475–485, 2000, doi: 10.1002/1099-1638(200011/12)16:6<475::AID-QRE342>3.0.CO;2-0.
[22] T. Goyal, R. S. Walia, and T. S. Sidhu, “Multi-response optimization of low-pressure cold-sprayed coatings through Taguchi method and utility concept,” *Int J Adv Manuf Technol*, vol. 64, no. 5, pp. 903–914, Feb. 2013, doi: 10.1007/s00170-012-4049-8.
[23] S. Kumar and K. Murugesan, “Optimization of geothermal interaction of a double U-tube borehole heat exchanger for space heating and cooling applications using Taguchi method and utility concept,” *Geothermics*, vol. 83, p. 101723, Jan. 2020, doi: 10.1016/j.geothermics.2019.101723.
[24] N. Pandey, K. Murugesan, and H. R. Thomas, “Optimization of ground heat exchangers for space heating and cooling applications using Taguchi method and utility concept,” *Applied Energy*, vol. 190, pp. 421–438, Mar. 2017, doi: 10.1016/j.apenergy.2016.12.154.
[25] Y. Xie, P. Hu, F. Lei, N. Zhu, and L. Xing, “Parameters optimization of ground source heat pump system combined energy consumption and economic analysis using Taguchi method,” in *Proceedings of the IGSHPA Research Track 2018*, International Ground Source Heat Pump Association, Sep. 2018, pp. 1–15. doi: 10.22488/okstate.18.000047.
[26] T. Sivasakthivel, K. Murugesan, and H. R. Thomas, “Optimization of operating parameters of ground source heat pump system for space heating and cooling by Taguchi method and utility concept,” *Applied Energy*, vol. 116, pp. 76–85, Mar. 2014, doi: 10.1016/j.apenergy.2013.10.065.
[27] T. Sivasakthivel, K. Murugesan, and P. K. Sahoo, “Optimization of ground heat exchanger parameters of ground source heat pump system for space heating applications,” *Energy*, vol. 78, pp. 573–586, Dec. 2014, doi: 10.1016/j.energy.2014.10.045.
[28] V. Verma and K. Murugesan, “Optimization of solar assisted ground source heat pump system for space heating application by Taguchi method and utility concept,” *Energy and Buildings*, vol. 82, pp. 296–309, Oct. 2014, doi: 10.1016/j.enbuild.2014.07.029.
[29] Modelica Association, “Modelica Language,” 2021. https://modelica.org/modelicalanguage.html (accessed Sep. 02, 2021).
[30] Dassault Systèmes, “Dymola,” 2022. https://www.3ds.com/products-services/catia/products/dymola/ (accessed May 23, 2022).

https://doi.org/10.52202/069564-0070

[31] Claytex Technia Company, “Thermal Systems Library & TIL Suite.” 2022. Accessed: May 23, 2022. [Online]. Available: https://www.claytex.com/products/dymola/model-libraries/thermal-systems-library/
[32] J. Formhals, H. Hemmatabady, B. Welsch, D. O. Schulte, and I. Sass, “A Modelica Toolbox for the Simulation of Borehole Thermal Energy Storage Systems,” *Energies*, vol. 13, no. 9, Art. no. 9, Jan. 2020, doi: 10.3390/en13092327.
[33] Lawrence Berkeley National Laboratory, “Modelica Buildings library.” Berkley, May 31, 2022. Accessed: Oct. 17, 2022. [Online]. Available: https://simulationresearch.lbl.gov/modelica/index.html
[34] L. Dai, S. Li, L. DuanMu, X. Li, Y. Shang, and M. Dong, “Experimental performance analysis of a solar assisted ground source heat pump system under different heating operation modes,” *Applied Thermal Engineering*, vol. 75, pp. 325–333, Jan. 2015, doi: 10.1016/j.applthermaleng.2014.09.061.
[35] S. H. Razavi, R. Ahmadi, and A. Zahedi, “Modeling, simulation and dynamic control of solar assisted ground source heat pump to provide heating load and DHW,” *Applied Thermal Engineering*, vol. 129, pp. 127–144, Jan. 2018, doi: 10.1016/j.applthermaleng.2017.10.003.
[36] Health and Safety Executive UK, “Managing legionella in hot and cold water systems,” 2022. https://www.hse.gov.uk/healthservices/legionella.htm (accessed Nov. 14, 2022).
[37] ASHRAE, “EnergyPlus Weather Data (Bergen).” 2001. Accessed: Oct. 17, 2022. [Online]. Available: Deutsches Institut für Normung
[38] J. Stene, “Residential CO2 Heat Pump System for Combined Space Heating and Hot Water Heating,” Fakultet for ingeniørvitenskap og teknologi, 2004. Accessed: May 23, 2022. [Online]. Available: https://ntnuopen.ntnu.no/ntnu-xmlui/handle/11250/233381
[39] J. Stene, “Residential CO2 heat pump system for combined space heating and hot water heating,” *International Journal of Refrigeration*, vol. 28, no. 8, pp. 1259–1265, Dec. 2005, doi: 10.1016/j.ijrefrig.2005.07.006.
[40] J. Stene, “Ground-source heat pump systems in Norway IEA HPP Annex 29 (2004-2006),” Norway, NEI-NO--0706407, 2007. [Online]. Available: https://inis.iaea.org/search/search.aspx?orig_q=RN:38097084
[41] K. Midttømme, “Geothermal Energy in Norway and Hordaland,” Bergen Energy Lab, 06 2017. [Online]. Available: https://www.uib.no/en/energy/108628/kirsti-midtt%C3%B8mme-geothermal-energy-norway-and-hordaland
[42] J. A. Duffie and W. A. Beckman, *Solar Engineering of Thermal Processes*, 4th ed. New Jersey: John Wiley & Sons, Inc., 2013. [Online]. Available: https://onlinelibrary.wiley.com/doi/pdf/10.1002/9781118671603.fmatter
[43] Deutsches Institut für Normung, “DIN EN 12975-1:2011-01 Thermal solar systems and components - Solar collectors - part 1: General requirements.” Jan. 2011.
[44] TUV Rheinland DIN CERTCO, “DIN CERTCO - Registration Number 011-7S094 F: Summary of EN 12975 Test Results.” 2014. Accessed: Oct. 18, 2022. [Online]. Available: https://www.dincertco.tuv.com/registrations/60064975?locale=en
[45] R. Valančius, A. Jurelionis, R. Jonynas, V. Katinas, and E. Perednis, “Analysis of Medium-Scale Solar Thermal Systems and Their Potential in Lithuania,” *Energies*, vol. 8, no. 6, Art. no. 6, Jun. 2015, doi: 10.3390/en8065725.
[46] B. Badenes, M. Á. Mateo Pla, T. Magraner, J. Soriano, and J. F. Urchueguía, “Theoretical and Experimental Cost–Benefit Assessment of Borehole Heat Exchangers (BHEs) According to Working Fluid Flow Rate,” *Energies*, vol. 13, no. 18, Art. no. 18, Jan. 2020, doi: 10.3390/en13184925.
[47] F. Mauthner and S. Herkel, *IEA SHC Task52 - Deliverable C1: Classification and benchmarking of solar thermal systems in urban environments*. 2017. doi: 10.13140/RG.2.2.31437.28648.
[48] Y. Wang, S. Zong, Y. Song, F. Cao, Y. He, and Q. Gao, “Experimental and techno-economic analysis of transcritical CO2 heat pump water heater with fin-and-tube and microchannel heat exchanger,” *Applied Thermal Engineering*, vol. 199, p. 117606, Nov. 2021, doi: 10.1016/j.applthermaleng.2021.117606.
[49] Quintel, “Cost of capital | Energy Transition Model,” 2023. https://docs.energytransitionmodel.com/main/cost-wacc/ (accessed Feb. 17, 2023).
[50] Statistics Norway, “09387: Electricity price, grid rent and taxes for households, by contents and quarter. Statbank Norway,” *SSB*, 2023. https://www.ssb.no/en/system/ (accessed Feb. 17, 2023).
[51] IEA, “Levelized cost of heating (LCOH) for consumers, for selected space and water heating technologies and countries,” *IEA*, 2022. https://www.iea.org/data-and-statistics/charts/levelized-cost-of-heating-lcoh-for-consumers-for-selected-space-and-water-heating-technologies-and-countries (accessed Feb. 23, 2023).
[52] C. Xi, L. Lin, and Y. Hongxing, “Long term operation of a solar assisted ground coupled heat pump system for space heating and domestic hot water,” *Energy and Buildings*, vol. 43, no. 8, pp. 1835–1844, Aug. 2011, doi: 10.1016/j.enbuild.2011.03.033.